Matter

CellPress

Article

Conformal three-dimensional interphase of Li metal anode revealed by low-dose cryoelectron microscopy

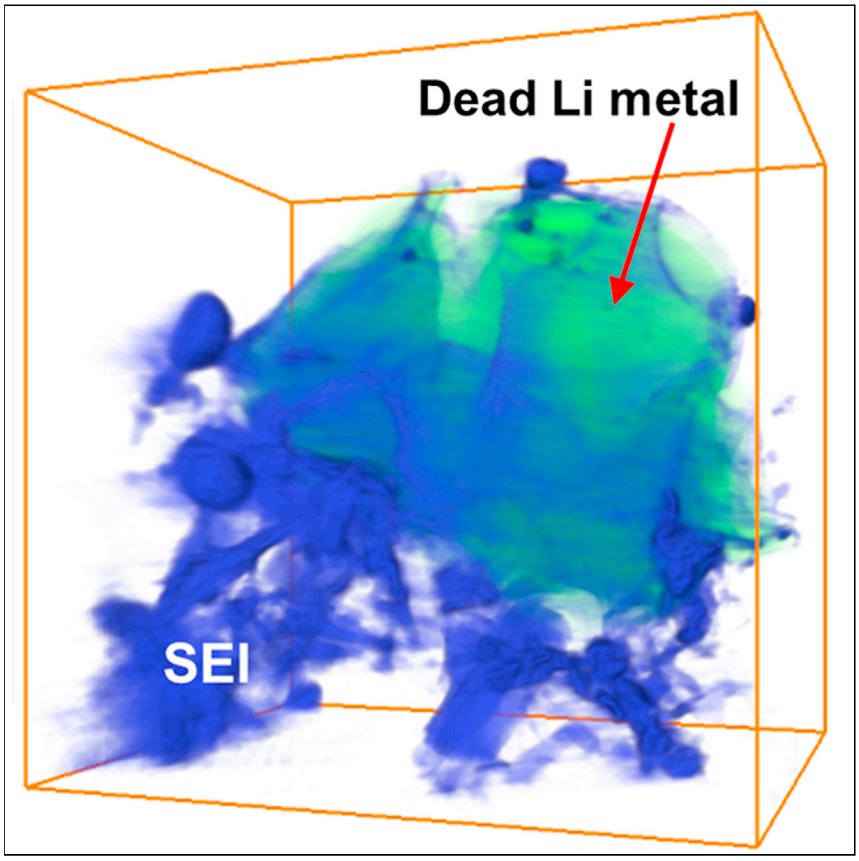

The cells cycled under accurately controlled uniaxial pressure can further enhance the repeated utilization of the SEI framework and improve the Coulombic efficiency (CE) to ~97%, demonstrating an effective strategy for reducing the formation of inactive "dead" Li and large quantities of additional SEI. The identification of such a flexible and porous 3D SEI framework clarifies the working mechanism of SEI in lithium metal batteries.

Bing Han, Xiangyan Li, Shuang Bai, ..., Zhi Chang, Ying Shirley Meng, Meng Gu

shirleymeng@ucsd.edu (Y.S.M.)
gum@sustech.edu.cn (M.G.)

Highlights

Using cryo-STEM tomography, we reveal the 3D structure of the SEI and dead lithium

The flexibility of SEI plays a vital role in preserving an SEI 3D framework

Our optimized uniaxial pressure greatly reduced the formation of new SEI and "dead" Li

3 **Understanding**
Dependency and conditional studies on material behavior

Han et al., Matter 4, 1–12
November 3, 2021
https://doi.org/10.1016/j.matt.2021.09.019

Please cite this article in press as: Han et al., Conformal three-dimensional interphase of Li metal anode revealed by low-dose cryoelectron microscopy, Matter (2021), https://doi.org/10.1016/j.matt.2021.09.019

Matter

CellPress

Article

Conformal three-dimensional interphase of Li metal anode revealed by low-dose cryoelectron microscopy

Bing Han,[1,7] Xiangyan Li,[1,4,7] Shuang Bai,[2] Yucheng Zou,[1] Bingyu Lu,[3] Minghao Zhang,[3] Xiaomin Ma,[5] Zhi Chang,[6] Ying Shirley Meng,[2,3,*] and Meng Gu[1,8,*]

SUMMARY

Using cryogenic transmission electron microscopy, we revealed three-dimensional (3D) structural details of the electrochemically plated lithium (Li) flakes and their solid electrolyte interphase (SEI). As the SEI skin layer is largely composed of nanocrystalline LiF and Li_2O in amorphous polymeric matrix, when complete Li stripping occurs, the compromised SEI 3D framework buckles and wrinkles. The flexibility and resilience of the SEI skin layer plays a vital role in preserving an intact SEI 3D framework after Li stripping. The intact SEI network enables the nucleation and growth of newly plated Li inside the previously formed SEI network in subsequent cycles, preventing additional large amounts of SEI formation. In addition, cells cycled under the accurately controlled uniaxial pressure can further enhance the repeated utilization of the SEI and improve the Coulombic efficiency (CE) by up to 97%, demonstrating an effective strategy for reducing the formation of additional SEI and inactive "dead" Li.

INTRODUCTION

SEI has been heavily researched in the past few decades due to its importance in extending Li-ion battery life and capacity retention.[1–3] The dynamic growth and fracturing of the SEI during battery cycling is closely correlated with the reactions between the electrolyte solutions and the electrode surfaces.[4–8] Ideally, the SEI should be formed during the initial cycles and then serve as a barrier between the bulk Li and the electrolyte solution, in favor of preventing continuous consumption of the Li ions and electrolyte solution in the subsequent cycles. Consequently, many researchers have tried to optimize the composition of electrolytes to form a stable and uniform thin passivating SEI on the anodes. However, previous studies on the SEI are heavily reliant on spectroscopic techniques, such as X-ray photoelectron spectroscopy, tip-enhanced Raman,[9] nuclear magnetic resonance,[10] and other advanced electroanalytical methods.[11–14] For example, Peled et al. depict a mosaic SEI structure, where the inorganic SEI components (nanosized Li_2O, LiF, Li_2CO_3, etc.) seem to be assembled randomly on the anode surface. To determine whether these SEI arrangements are randomly formed or driven by a yet unseen mechanism, analytical techniques with high spatial resolution are needed to accurately probe the identity and distributions of these nano phases. However, due to the fact that the SEI samples are extremely sensitive to air and probing sources, such as electron beams, accurate measurement of the composition, component distribution, and morphology of the SEI at the atomic scale is rarely reported, not to mention the three-dimensional (3D) information. To gain better insight into the failure

Progress and potential

With applied uniaxial stack pressure, a stable and porous 3D SEI network allows for fast Li^+ transport and the nucleation of newly plated Li metal without the formation of large quantities of additional SEI. In addition, the identification of such a flexible and porous 3D SEI framework clarifies the working mechanism of SEI in lithium metal anodes for batteries. The insights provided in this work will inspire researchers to design more functional artificial 3D SEI on other metal anodes to improve rechargeable metal batteries with long cycle life.

Please cite this article in press as: Han et al., Conformal three-dimensional interphase of Li metal anode revealed by low-dose cryoelectron microscopy, Matter (2021), https://doi.org/10.1016/j.matt.2021.09.019

mechanisms of Li metal anodes, we need a clearer map of SEI evolution at different charge and discharge states; this will help us to further understand the role of SEI layers and their relation to the performance of the Li metal anode.

Because of the fragility of the liquid-solid interfaces in Li metal anodes, the best option for atomic-scale SEI characterization is cryogenic aberration-corrected transmission electron microscopy (cryo-TEM).[3,15–18] Using this method, Wang et al. revealed the nucleation process of Li metal, and demonstrated that glassy Li metal is more favorable in electrochemical reversibility;[17] Cui and colleagues reported distinct mosaic and multilayer types of SEI that form on the Li metal anode after cycling with pure ethylene carbonate (EC)/diethyl carbonate (DEC) and fluoroethylene carbonate (FEC)-modified EC/DEC electrolytes, respectively, and demonstrated that FEC modification dramatically improves battery performance.[19,20] Cryo-electron energy loss spectroscopy mapping (EELS) has also revealed the possible formation of the LiH phase in plated Li metal, which may reduce the cycling capability of Li metal anodes.[18] The SEI skin layer generally contains two crucial types of components: inorganic crystalline grains and an organic, amorphous polymeric matrix.[21] The distribution of inorganic components inside the polymeric matrix plays a critical role in dictating the ionic and electronic conductivity[22] and mechanical stability of the SEI, and thus the cyclability of the Li metal anode. The ideal SEI skin layer maintains integrity by resilient accommodations to the volume changes of the anode materials during many cycles of Li plating and stripping. The mechano-chemical properties, resistance, ionic conductivity, and recyclability of the SEI urgently need precise characterization at high resolution in real space.[19,23–25] However, limited studies in the literature have revealed the atomic structure, leaving a predominantly unknown domain for research. The morphology and structure of the SEI after Li deposition and stripping need to be further studied at the atomic scale and three dimensions using cryo-TEM in order to accurately correlate its structure-property with Li metal cyclability.

RESULTS AND DISCUSSION

The LiF component in the SEI in FEC-modified EC/DEC is believed to be the primary factor for enhanced performance. However, its form and distribution is heavily debated in the field. Li et al. did not find LiF in their study,[20] while others report the identification and important roles of LiF in stabilizing the SEI.[26–28] We believe that the electron dosage plays a vital role in accurately imaging the native state of the SEI on Li metal. Therefore, we have developed a low-dose technique to allow for the acquisition of high-resolution TEM (HRTEM) images with only 80 e $Å^{-2}$, compared with the 30,000 e $Å^{-2}$ chosen in the Li et al. study.[20] We focused our study on the higher-performing FEC-modified EC/DEC electrolyte solution. We characterized the same sample from the micron-scale down to the atomic scale, revealing that the as-plated Li metal exhibits flake morphology ranging from a few hundred nanometers to 10 μm in Figures 1A–1C. The FEC additive induces the formation of a uniformly thin SEI layer (~25 nm) on the Li metal (Figure 1B) with the LiF nanocrystals distributed in the inner layer of the SEI skin (Figures 1C–1E). The HRTEM image in Figure 1D clearly shows the {002} set of planes of LiF. At the same time, large quantities of Li_2O were found in the surficial SEI skin as shown in Figure 1F. The nanocrystalline LiF and Li_2O islands are distributed randomly inside the amorphous polymeric matrix, which forms the general morphology of the insulating SEI skin. In contrast, the SEI formed in pure EC/DEC is very non-uniform with large variation in thickness, and is composed of mostly Li_2O and Li_2CO_3 components, as shown in Figure S1. The Li_2CO_3 component is unstable against the electrolyte and will decompose to form

[1]Department of Materials Science and Engineering, Southern University of Science and Technology, Shenzhen 518055, China

[2]Materials Science and Engineering, University of California San Diego, La Jolla, CA, USA

[3]Department of Nano Engineering, University of California San Diego, La Jolla, CA, USA

[4]Academy for Advanced Interdisciplinary Studies, Southern University of Science and Technology, Shenzhen 518055, China

[5]Cryo-TEM Center, Southern University of Science and Technology, Shenzhen 518055, China

[6]Energy Technology Research Institute, National Institute of Advanced Industrial Science and Technology (AIST), Tsukuba 305-8568, Japan

[7]These authors contributed equally

[8]Lead contact

*Correspondence: shirleymeng@ucsd.edu (Y.S.M.), gum@sustech.edu.cn (M.G.)

https://doi.org/10.1016/j.matt.2021.09.019

Please cite this article in press as: Han et al., Conformal three-dimensional interphase of Li metal anode revealed by low-dose cryoelectron microscopy, Matter (2021), https://doi.org/10.1016/j.matt.2021.09.019

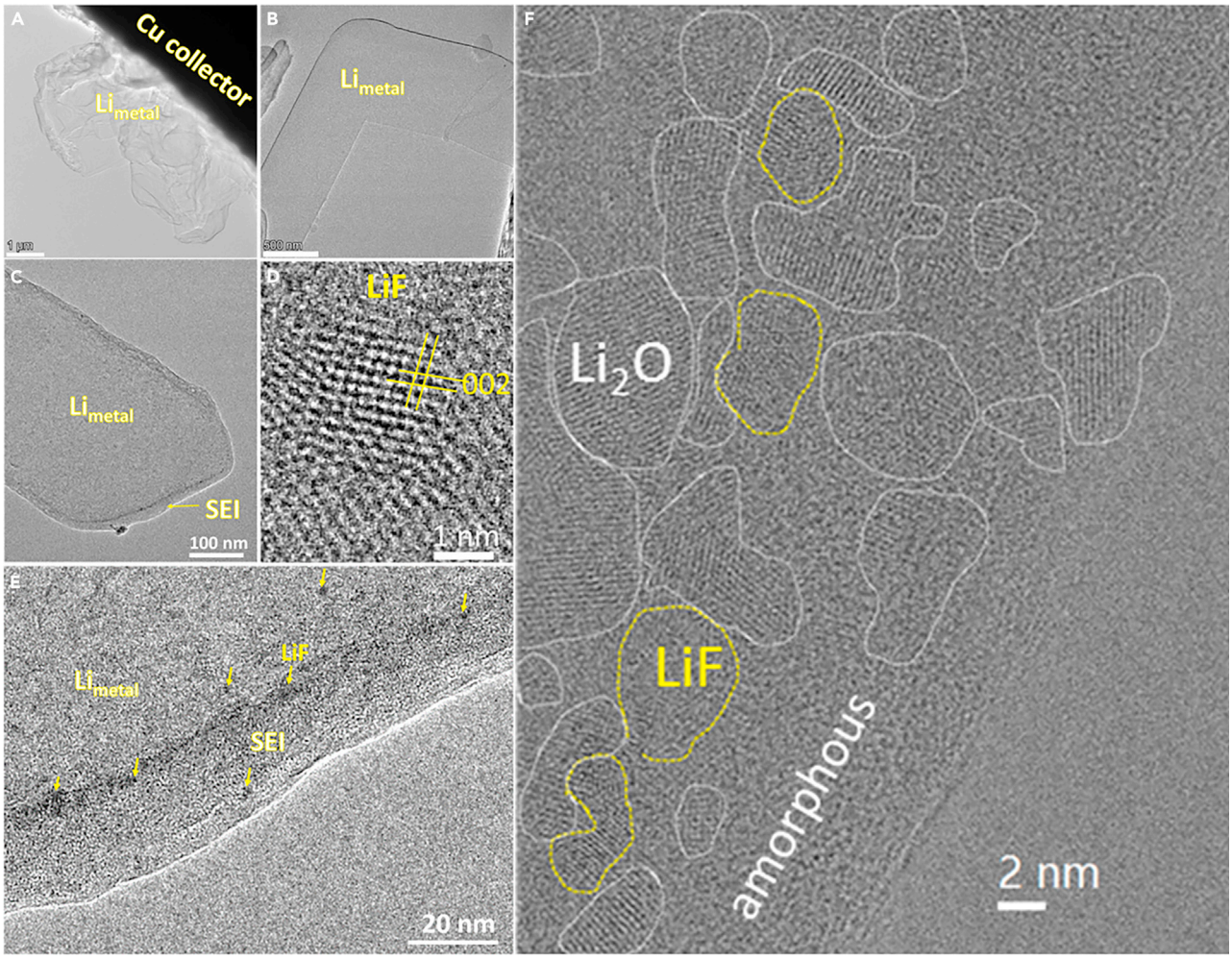

Figure 1. Cryo-TEM analysis of the plated Li flake and SEI formed using FEC additive after the first plating process

(A–C) Low-magnification cryo-TEM images showing plated Li metal and its SEI.

(D) HRTEM showing the LiF nanocrystal inside the SEI.

(E) Magnified local region showing the dark LiF nanocrystals (indicated by yellow arrows) inside the SEI.

(F) Distribution map of different phases in the SEI skin layer.

The HRTEM images in (D and F) were acquired with an electron dose rate of ~8 e $Å^{-2}$ s^{-1} for ~10 s.

gaseous species.[21] Therefore, the addition of FEC can induce a uniformly thin SEI layer with more stable LiF inorganic crystals and minimize unstable Li_2CO_3 component.[21]

The combination of our cryogenic scanning transmission electron microscopy (cryo-STEM) and cryo-EELS results offer unprecedented insight into the chemical composition of the SEI skin layer after just the first plating cycle. As shown by the large-scale cryo-STEM images in Figure 2A, there is a high density of bright clusters (indicated by white arrows) against the dark Li matrix, demonstrating local enrichment of impurities. The cryo-EELS elemental maps in Figures 2B–2F also detect Li, oxygen (O), fluorine (F), and carbon (C) signals inside the Li matrix. We speculate that the presence of the impurities (including fluorine, carbon, and possibly oxygen) is one of the important factors that induce amorphization of some local regions of the plated Li because the local fluctuation and enrichment of these impurities leads to the formation of nanocrystalline Li_2O, and LiF (which may break SEI skin layers into pieces)

Please cite this article in press as: Han et al., Conformal three-dimensional interphase of Li metal anode revealed by low-dose cryoelectron microscopy, Matter (2021), https://doi.org/10.1016/j.matt.2021.09.019

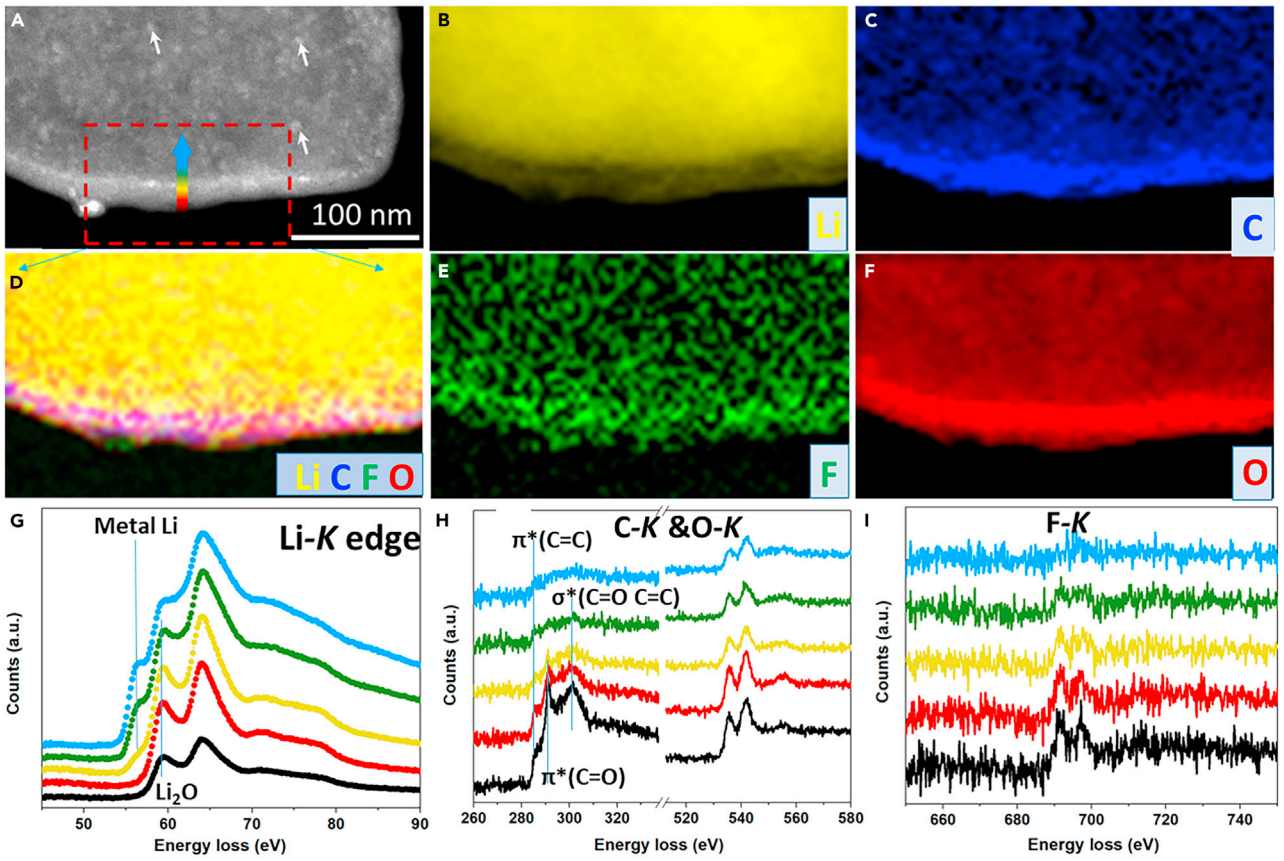

Figure 2. STEM EELS analysis of the plated Li metal and its SEI

(A) STEM image showing the region of the EELS map (red rectangle) and line profile (arrow).

(B–F) EELS elemental maps of (B) Li, (C) C, (D) composite, (E) F, and (F) O.

(G) Li *K* edge.

(H) C *K* and O *K* edges.

(I) F *K* edge from the line profile along the arrow from the surface to the inside of the Li metal. Scale bars, 100 nm (A–F).

randomly buried inside the Li matrix during the electrochemical cycling. These EELS elemental maps correspond with the HRTEM image shown in Figure 1F, which shows the presence of Li_2O and LiF nano-islands inside the plated Li matrix. The EELS line profiles indicate that, when scanning from the surface to the bulk, the intensity of the peaks of the elements (F, O, and C) has an obvious high-to-low trend (Figures 2H and 2I). The simultaneous increase of metallic Li and the decrease of the elements, such as F, O, and C, strongly suggests that SEI elements have been doped into the plated Li metal matrix. The same cryo-EELS fine structure analysis also shows that the amorphous polymeric matrix contains large amounts of carbonate groups (–O–(C=O)–O–) (Figure 2H). Furthermore, previous literature also indicates that SEI formed using the FEC-containing electrolyte contains mostly crosslinked (ethylene oxide) (PEO) and aliphatic chains along with carbonate and carboxylate species,[10] which is consistent with our EELS analysis. The SEI skin layer contains oxidized Li, while the inner Li bulk exhibits more metallic fine structure of Li *K* (Figures 2G and 2H), and the SEI skin layer has a strong F signal, while the inner matrix has a relatively weak F signal (Figure 2I). Therefore, the elemental content between the plated Li metal and SEI skin are not as distinct as we generally speculated.[4]

Please cite this article in press as: Han et al., Conformal three-dimensional interphase of Li metal anode revealed by low-dose cryoelectron microscopy, Matter (2021), https://doi.org/10.1016/j.matt.2021.09.019

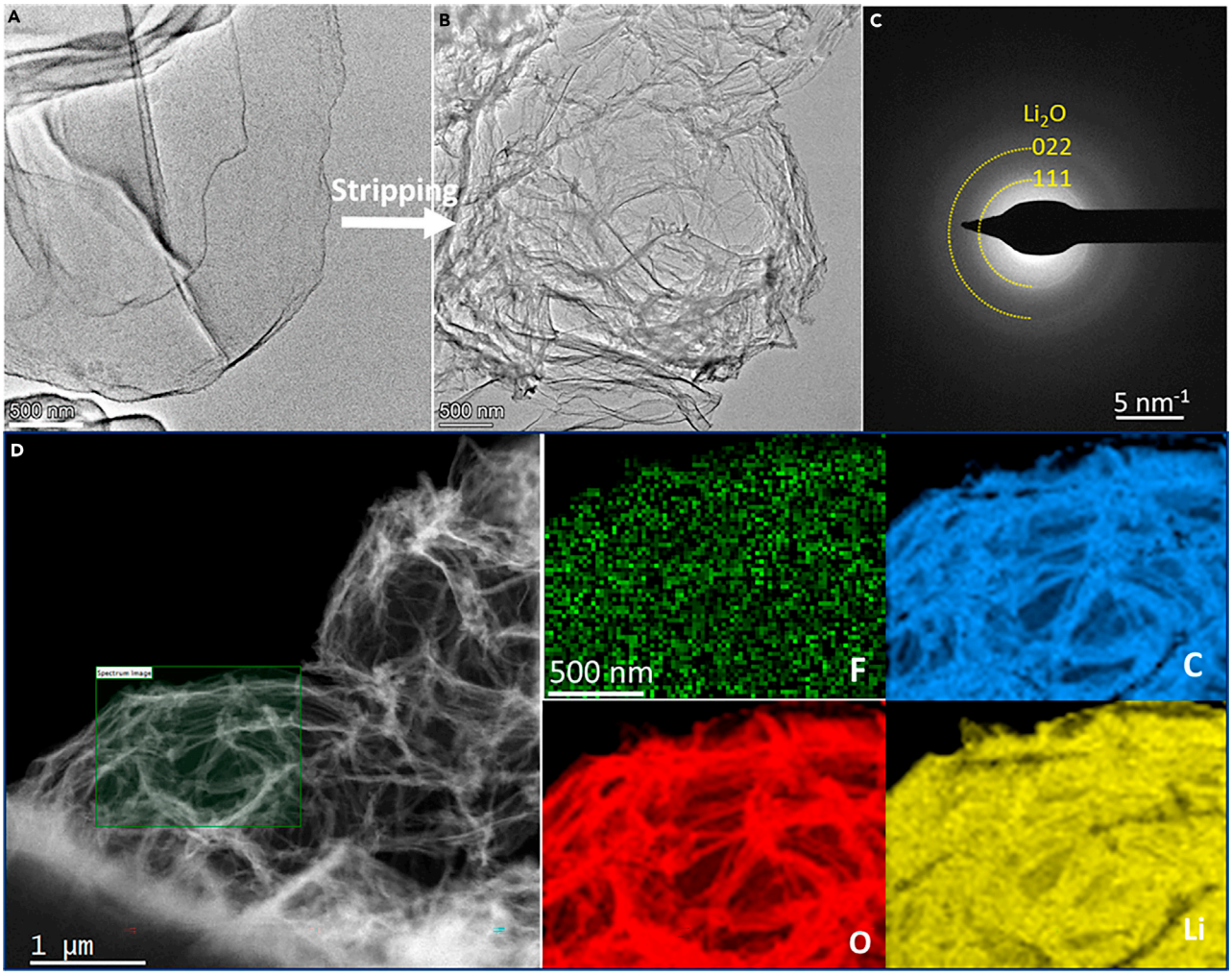

Figure 3. The morphology of the SEI after the first stripping cycle

(A) Cryo-TEM image of the as-plated Li.

(B) Morphology of the remaining empty husks after the first stripping cycle.

(C) Electron diffraction of the remaining empty husks after Li stripping.

(D) Cryo-STEM image and EELS elemental maps (green, fluorine; blue, carbon; red, oxygen; yellow, Li) of the empty husks.

The SEI skin acts as a protective layer for the plated Li metal, preventing further reaction between the electrolyte and the Li metal. The estimated electron tunneling distances may be as short as 2–3 nm for perfectly compacted inorganic SEI components (such as Li_2O, LiF, or Li_2CO_3), as predicted by density functional theory calculations.[29,30] However, even though the as-formed SEI is a composite of both inorganic crystals and organic components and may contain structural defects, a 20–30-nm-thick SEI skin should predominantly prevent electron leakage and protect the deposited Li metal.

To evaluate the structural robustness of the SEI skin layer, we probed the morphology of the SEI after the first stripping cycle (Figure 3). The filled SEI skin layer containing large flakes of the plated Li metal (Figure 3A) contrasts sharply with the empty, deflated, and empty SEI husks in (Figure 3B). Interestingly, the process of Li stripping caused the empty SEI husks to shrink without complete collapse, which indicates that the mechanical strength of the SEI allows it to survive large volume

Please cite this article in press as: Han et al., Conformal three-dimensional interphase of Li metal anode revealed by low-dose cryoelectron microscopy, Matter (2021), https://doi.org/10.1016/j.matt.2021.09.019

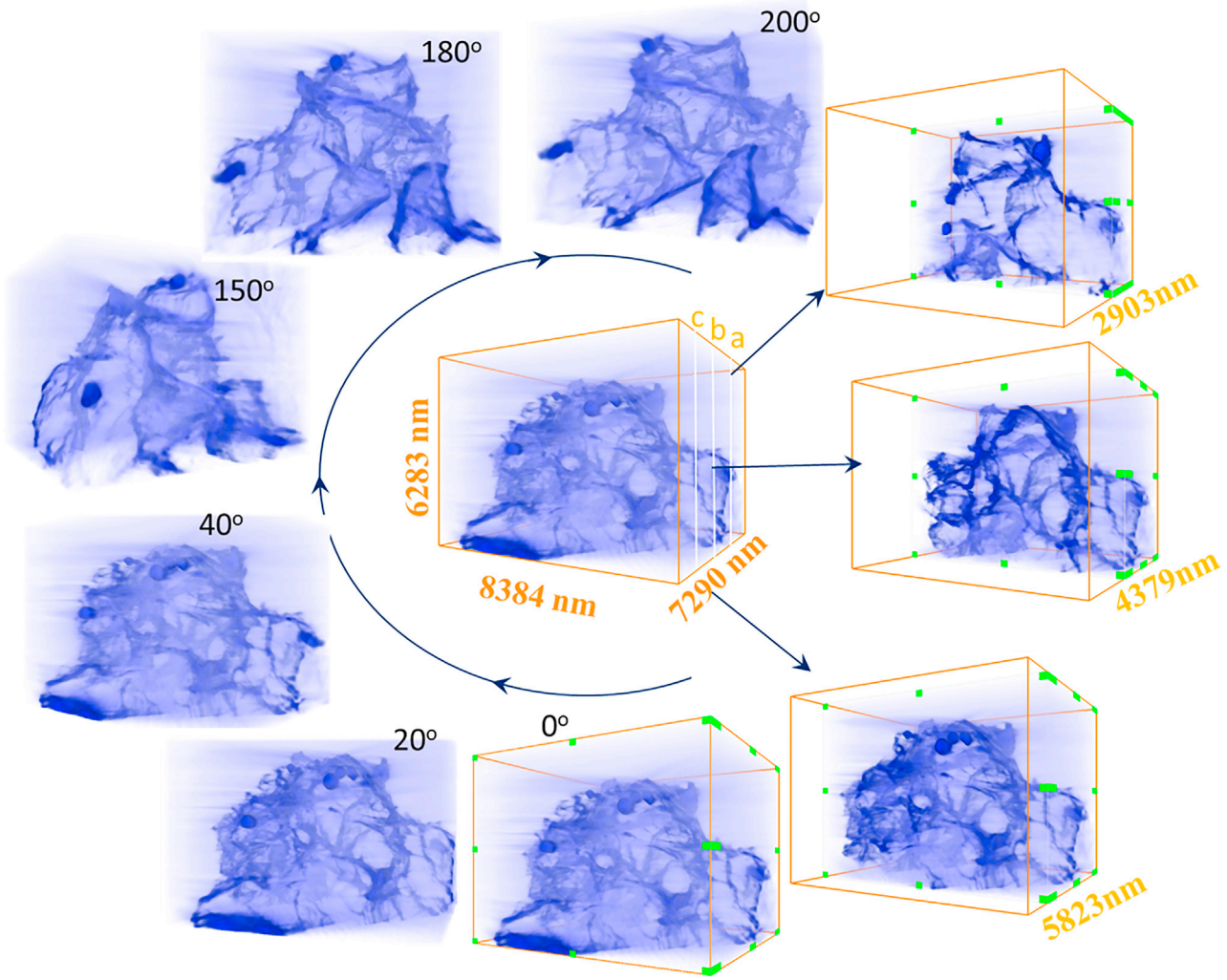

Figure 4. STEM tomography reconstructed the 3D image of the SEI husk after Li stripping, illustrating the hollow, crumpled SEI structure

The left images (0°–200°) show the SEI husks viewed from different angles; while the images on the right side (boxed in orange) show cross-sections the SEI husks at positions of "a" 2,903 nm, "b" 4,379 nm, and "c" 5,823 nm (marked by the white lines in the central image). (For the complete tilt series, 0°–360° rotational view, and cross-section slicing, please refer to Videos S1, S2, and S3.)

changes, probably because of the flexibility of the organic/polymeric matrix in the SEI skin layer. While the study by Li et al. demonstrated the importance of having an electrolyte solution (FEC additive) that can lead to an organic/polymeric matrix in the SEI skin layer, our characterization explains *why* those components are so critical. The selected area electron diffraction pattern further indicates that Li_2O is the dominating inorganic component of the empty SEI husks in Figure 3C. The high-angle annular dark-field (HAADF) STEM images and elemental maps in Figure 3D shows the content of F, C, O, and Li in the empty SEI husks. These results are in good agreement with the previously identified Li_2O and LiF nanocrystalline regions in the SEI.

To visualize the 3D structure of the SEI network more clearly, we performed a cryo-STEM tomography tilt series in a 0°–100° range (Figure S2; Video S1) to fully reveal the empty SEI husk network. We also displayed the reconstructed 3D SEI network from 0° to 360° angles (Video S2) and in a cross-section slicing video (Video S3).

Please cite this article in press as: Han et al., Conformal three-dimensional interphase of Li metal anode revealed by low-dose cryoelectron microscopy, Matter (2021), https://doi.org/10.1016/j.matt.2021.09.019

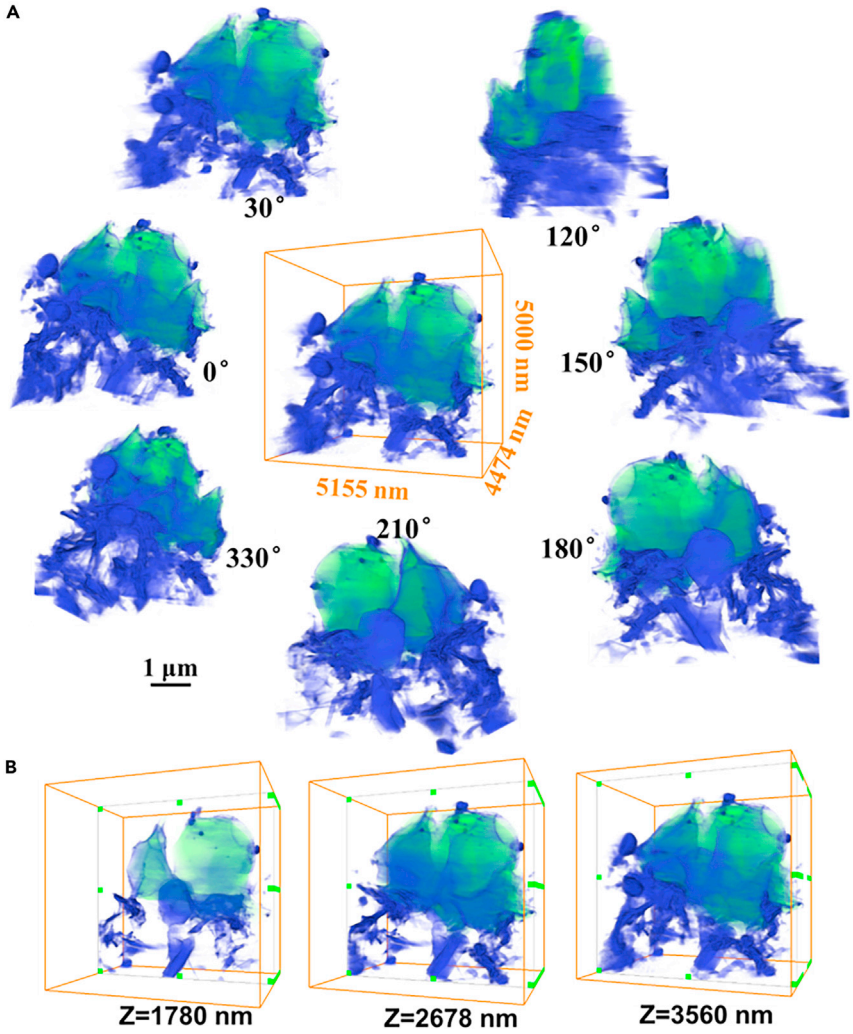

Figure 5. STEM tomography reconstructed 3D image of the dead Li (highlighted in green) after Li stripping

(A) A 0°–360° view showing the dead Li particle viewed from different angles.

(B) Cross-section views at different positions on the z axis (1,780, 2,678, and 3,560 nm). (For a better visualization, please refer to Videos S4 and S5.)

Figure 4 illustrates the empty SEI husks at selected viewing angles and cross-section slices. As clearly shown by the tilt series and reconstructed 3D videos, the buckled SEI husks remain intact but porous after Li stripping (see also Figure S3 for smaller but deflated SEI husks). The flexibility of the amorphous SEI matrix allows the SEI to fold, and bend during the stripping, which preserve the intact frameworks of the SEI. The crosslinked polymeric phase in the SEI skin layer keeps the SEI framework intact during Li plating by resiliently cushioning the volume changes during stripping and plating a flexibility that is largely correlated with both good capacity retention and high Coulombic efficiency (CE).[31,32]

In addition to identifying the empty SEI husks after Li stripping, 3D STEM tomography also helps to accurately locate the presence of dead Li (highlighted in green) in Figure 5. The 0°–360° view in Figures 5A and Video S4 clearly shows that the dead Li particle (~4 μm) sits on top of the empty SEI husks and its electron conduction path is

Please cite this article in press as: Han et al., Conformal three-dimensional interphase of Li metal anode revealed by low-dose cryoelectron microscopy, Matter (2021), https://doi.org/10.1016/j.matt.2021.09.019

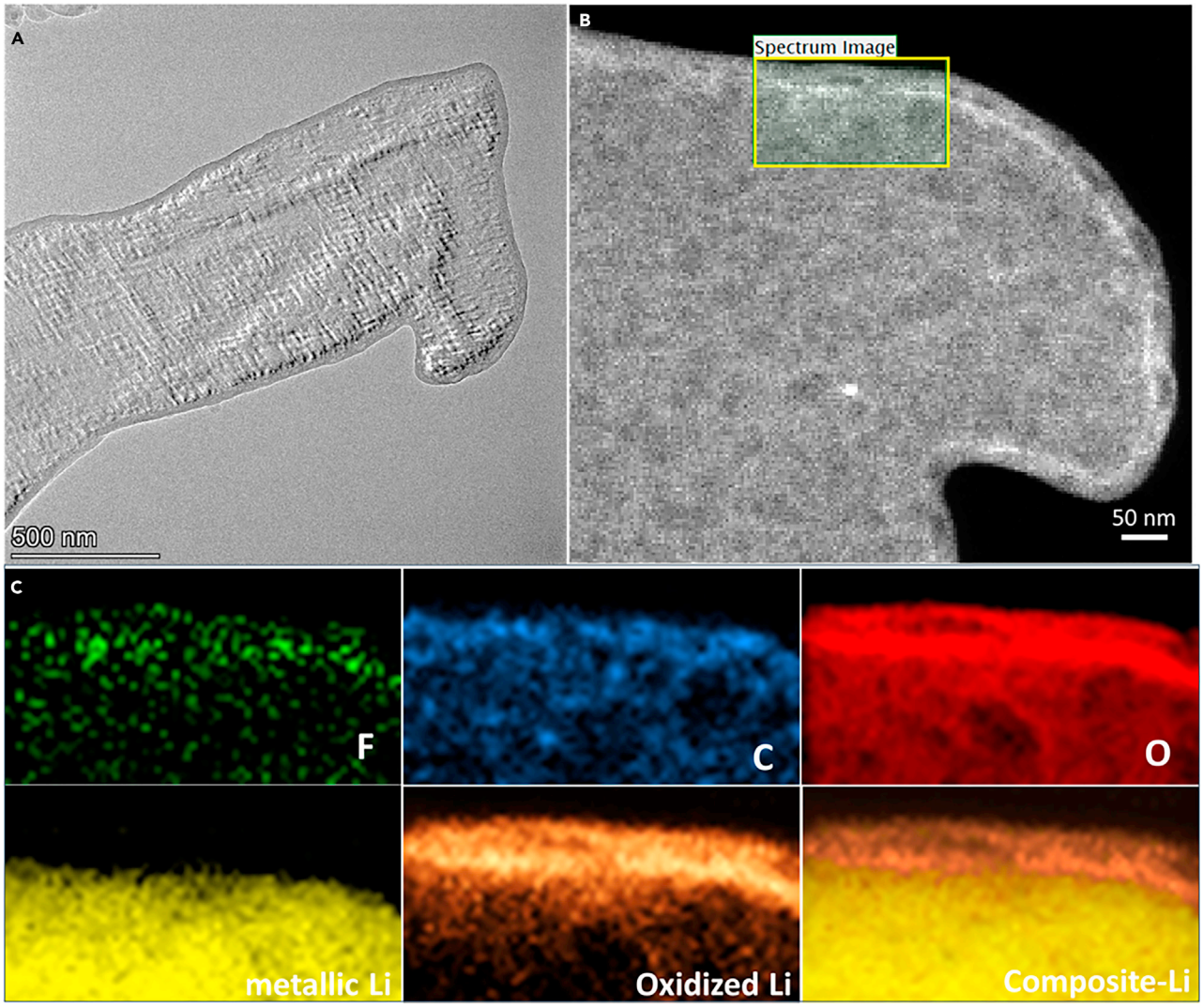

Figure 6. The morphology of a new Li electrode after two lithiation cycles (the empty husks are reinflated by the newly plated Li)
(A) Cryo-TEM and (B) cryo-STEM image of the second round of plated Li metal.
(C) Elemental maps of F, C, O, metallic Li, oxidized Li, and composite Li map in the rectangular spectrum image region in (B).

cut off from the bottom part of the Li metal or the current collector. As a result, the Li atoms in this particle can no longer lose electrons to the current collector and become free Li^+ ions. Furthermore, the cross-sectional views in Figures 5B and Video S5 illustrate the morphology variations in the dead Li particle with changing cross-section slices and its connections with SEI husks below. In addition, Figure S4 in the supplemental information shows additional dead Li metal after just one stripping cycle due to likely non-uniform local stripping rates during the stripping cycle. Observations of the dead Li formation in 3D allows us to see the origin of dead Li, which is the primary reason why batteries lose capacity and deteriorate during cycling.[3]

We further note that the empty SEI husks form a perfect 3D network for the newly plated Li in the following cycle. To better understand how the Li refills the SEI husks, we analyzed a new Li electrode after two lithiation cycles. As anticipated, the empty husks are reinflated by the newly plated Li (Figures 6A and 6B). The HAADF STEM image and elemental maps in Figures 6B and 6C also show the presence of O, F,

Please cite this article in press as: Han et al., Conformal three-dimensional interphase of Li metal anode revealed by low-dose cryoelectron microscopy, Matter (2021), https://doi.org/10.1016/j.matt.2021.09.019

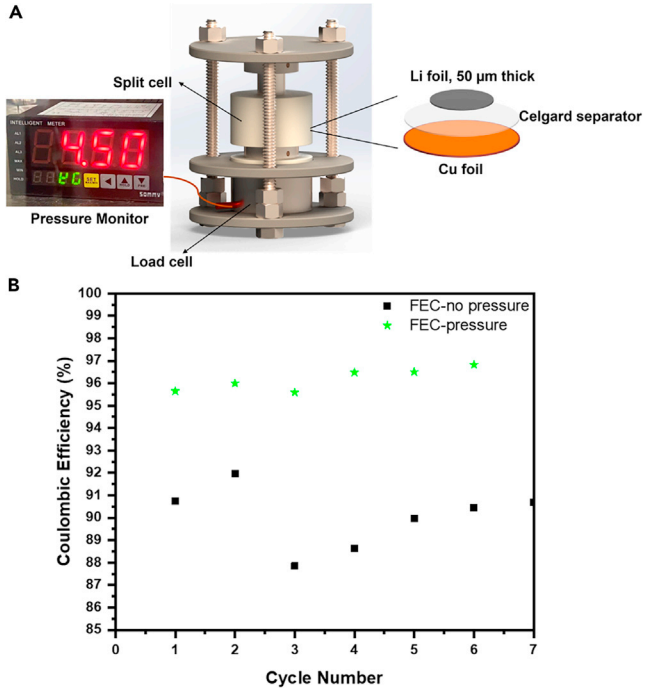

Figure 7. A split cell with precisely controlled uniaxial stack pressure (350 kPa) to increase the reusability of the SEI husks

(A) Schematic showing the pressure cell with precisely controlled uniaxial stack pressure (350 kPa) applied to the battery during cycling.

(B) Cycling CE of the pressure cell compared with no pressure using 1 M $LiPF_6$ electrolyte solutions with EC:DEC:FEC (20:70:10 by vol %).

and some carbon species inside the Li metal matrix.[21] The high contrast of O inside the Li matrix clearly indicates the formation Li_2O and the network-like distribution of Li_2O. Interestingly, we used multiple linear least-squares fitting to deconvolute the Li *K* edge to show the presence of metallic Li and oxidized Li in the EELS maps (Figure 6C). The SEI skin layer is rich in Li_2O, while the bulk Li metal primarily contains metallic Li, with only a small amount of Li_2O. Again, we see that the 3D SEI network allows Li to penetrate through the SEI, nucleate, and grow without forming new SEI. We also analyzed the empty SEI husks after 10 cycles, and found that the SEI could become deflated, but the integrity of the SEI husks was maintained, as shown by the 3D views and higher-magnification cryo-TEM micrographs in Figure S5.

The addition of FEC into the EC/DEC obviously enhances the electrochemical cycling performance of the Li metal anode to a large extent.[11,20,33,34] Our understanding of the 3D structure of SEI inspired us to further tailor the setup of the battery cell to optimize cycling performance. As observed in our experiments, the size distribution of the empty SEI husks is quite large, ranging from a few hundred nanometers to about 10 μm. Such large quantities of high-density, insulating SEI husks on the surface of the Li metal consequently leads to increased impedance of the cells after the first cycle. In addition, the formation of dead Li is clearly observed in Figure 5. Therefore, to facilitate the Li transport and re-deposition of Li into the empty SEI husks and minimize the formation of dead Li, we designed a split cell with precisely controlled uniaxial stack pressure (350 kPa) to increase the reusability of the SEI husks, as shown in Figure 7A.[35] An intimate contact with the current collector ensures Li to refill into the SEI husks. Our optimized uniaxial stack

Please cite this article in press as: Han et al., Conformal three-dimensional interphase of Li metal anode revealed by low-dose cryoelectron microscopy, Matter (2021), https://doi.org/10.1016/j.matt.2021.09.019

pressure greatly improved CE (Figure 7B) by 96% at the first cycle and 97% at the sixth cycle, vastly outperforming the same EC/DEC-FEC cell without pressure (CE ~87%–92%).

Conclusions

Cryo-STEM tomography is an effective tool for visualizing the atomic structure and 3D architecture of the SEI at different charge and discharge states. Using cryo-TEM, we demonstrated that a good (FEC additive) electrolyte solution induces the formation of a 3D SEI network with a uniform organic/polymeric outer layer and a LiF-containing inner layer. Because the SEI inherits a flexible stretchable property from the organic SEI layer and a robust structure from the inner, inorganic SEI layer, the SEI husk crumples but does not collapse during delithiation. In fact, the SEI husk facilitates Li^+ transport, nucleation, and growth of Li in the next lithiation cycle because the flexible empty husk morphology allows Li to refill the SEI husks to limit the formation of new SEI layers. This characterization explains well-documented observations that the CE improves after the first cycle, during which the 3D SEI network forms.

In addition, we put a Li||Cu cell under accurately controlled stack pressure and demonstrated that a closer and intimate contact with the current collector allows the SEI husks to be more repeatedly utilized in the following cycles and further improved CE by up to 5%–9% in the cycling. Our study offers a successful example of the kind of improvement that this atomic-scale and 3D characterization can induce, while providing an exciting new analytical method for future SEI and other beam-sensitive materials.

EXPERIMENTAL PROCEDURES

Resource availability

Lead contact

Further information and requests for resources and materials should be directed to and will be fulfilled by the lead contact, Meng Gu (gum@sustech.edu.cn).

Materials availability

This study did not generate new unique materials.

Date and code availability

This study did not generate or analyze (datasets or code).

We assembled CR2032-type coin cells in an Ar-filled glovebox using Li metal as a counter electrode. We used 1 M $LiPF_6$ electrolyte solutions with EC:DEC:FEC (20:70:10 by vol %). A Cu-TEM grid was intentionally put on to the Cu surface in the working electrode. Some Li metal is deposited on the Cu-TEM grid during plating. The Li plating and stripping cycles are conducted with a constant current mode of 0.5 mA/cm^2 to a capacity of 0.5 mAh/cm^2. After cycling, we opened up the coin cells and took the Cu-TEM grid out to transfer into the TEM after rinsing with dimethyl carbonate (DMC) to remove residue salts and electrolytes. We used a Titan Krios with a Cs-aberration corrector operating at 300 kV. All TEM images were acquired at 77 K with an ultra-low dose of electrons (~7 e $Å^{-2}$ s^{-1} × 10 s) with a direct-detect device (Falcon 4). The low-magnification STEM used a low current of 11 pA and the dosage for STEM is around 200 e/nm^2. The cryo-EELS maps were acquired using 11 pA current with 0.1 s dwell time at each pixel and the EELS spectra are summed over a few pixels to enhance the signal-to-noise ratio.

Li-Cu split cell test: a customized split cell with a load cell was used to precisely control the uniaxial stack pressure (350 kPa) applied to the battery during cycling. The split cell consists of two parts: two titanium plungers and one polyether ether ketone (PEEK) die mold. The Cu||Li cells were assembled in an Ar-filled glovebox by sandwiching the Li metal foil (50 μm thick), Celgard separator, and the cleaned Cu foil between the two titanium plungers inside the PEEK die mold. Only a minimum amount of electrolyte (~5 μL) was added to the Cu||Li cells to wet the separator.

SUPPLEMENTAL INFORMATION

Supplemental information can be found online at https://doi.org/10.1016/j.matt.2021.09.019.

ACKNOWLEDGMENTS

This work was supported by the Shenzhen Natural Science Fund (Grant No. 20200925154115001) , Shenzhen Science and Technology Program (Grant No. KQTD20190929173815000), Guangdong Innovative and Entrepreneurial Research Team Program (Grant No. 2019ZT08C044), the Shenzhen DRC project [2018]1433, and Shenzhen Clean Energy Research Institute (no. CERI-KY-2019-003). This work was performed at the Pico and Cryo-TEM Center at SUSTech Core Research Facility. Y.S.M. acknowledges funding support from the Zable Endowed Chair of Energy Technology and the Sustainable Power & Energy Center of UC San Diego. S.B. is grateful for financial support from the Materials Science and Engineering Program of UC San Diego.

AUTHOR CONTRIBUTIONS

M.G. and Y.S.M. designed and supervised the experiments. B.H. and Y.Z. carried out the cryo-TEM and battery testing. X.L. did the tomography reconstruction. M.G., B.H., S.B., and M.Z. analyzed the data. All authors discussed and edited the paper.

DECLARATION OF INTERESTS

The authors declare no competing interests.

Received: May 28, 2021
Revised: August 2, 2021
Accepted: September 17, 2021
Published: October 18, 2021

REFERENCES

1. Peled, E., Golodnitsky, D., Ardel, G., and Eshkenazy, V. (1995). The SEI model—application to lithium-polymer electrolyte batteries. Electrochim. Acta *40*, 2197–2204.

2. Peled, E., Golodnttsky, D., Ardel, G., Menachem, C., Bar Tow, D., and Eshkenazy, V. (1995). The role of SEI in lithium and lithium ion batteries. MRS Proc. *393*, 209.

3. Fang, C., Li, J., Zhang, M., Zhang, Y., Yang, F., Lee, J.Z., Lee, M.-H., Alvarado, J., Schroeder, M.A., Yang, Y., et al. (2019). Quantifying inactive lithium in lithium metal batteries. Nature *572*, 511–515.

4. Peled, E., and Menkin, S. (2017). Review—SEI: past, present and future. J. Electrochem. Soc. *164*, A1703–A1719.

5. Parimalam, B.S., MacIntosh, A.D., Kadam, R., and Lucht, B.L. (2017). Decomposition reactions of anode solid electrolyte interphase (SEI) components with LiPF6. J. Phys. Chem. C *121*, 22733–22738.

6. Purushotham, U., Takenaka, N., and Nagaoka, M. (2016). Additive effect of fluoroethylene and difluoroethylene carbonates for the solid electrolyte interphase film formation in sodium-ion batteries: a quantum chemical study. RSC Adv. *6*, 65232–65242.

7. Kamikawa, Y., Amezawa, K., and Terada, K. (2020). Elastic–plastic deformation of a solid electrolyte interface formed by reduction of fluoroethylene carbonate: a nanoindentation and finite element analysis study. J. Phys. Chem. C *124*, 22488–22495.

8. Zhang, W., Cai, T.H., and Sheldon, B.W. (2019). The impact of initial SEI formation conditions on strain-induced capacity losses in silicon electrodes. Adv. Energy Mater. *9*, 1803066.

9. Nanda, J., Yang, G., Hou, T., Voylov, D.N., Li, X., Ruther, R.E., Naguib, M., Persson, K., Veith, G.M., and Sokolov, A.P. (2019). Unraveling the nanoscale heterogeneity of solid electrolyte interphase using tip-enhanced Raman spectroscopy. Joule *3*, 2001–2019.

10. Jin, Y., Kneusels, N.-J.H., Marbella, L.E., Castillo-Martínez, E., Magusin, P.C.M.M., Weatherup, R.S., Jónsson, E., Liu, T., Paul, S., and Grey, C.P. (2018). Understanding fluoroethylene carbonate and vinylene carbonate based electrolytes for Si anodes in lithium ion batteries with NMR spectroscopy. J. Am. Chem. Soc. *140*, 9854–9867.

11. Fondard, J., Irisarri, E., Courrèges, C., Palacin, M.R., Ponrouch, A., and Dedryvère, R. (2020). SEI composition on hard carbon in Na-ion batteries after long cycling: influence of salts (NaPF6, NaTFSI) and additives (FEC, DMCF). J. Electrochem. Soc. *167*, 070526.

12. Huang, W., Attia, P.M., Wang, H., Renfrew, S.E., Jin, N., Das, S., Zhang, Z., Boyle, D.T., Li, Y., Bazant, M.Z., et al. (2019). Evolution of the solid–electrolyte interphase on carbonaceous anodes visualized by atomic-resolution cryogenic electron microscopy. Nano Lett. *19*, 5140–5148.

13. Ji, L., Gu, M., Shao, Y., Li, X., Engelhard, M.H., Arey, B.W., Wang, W., Nie, Z., Xiao, J., Wang, C., et al. (2014). Controlling SEI formation on SnSb-porous carbon nanofibers for improved Na ion storage. Adv. Mater. *26*, 2901–2908.

14. Jurng, S., Brown, Z.L., Kim, J., and Lucht, B.L. (2018). Effect of electrolyte on the nanostructure of the solid electrolyte interphase (SEI) and performance of lithium metal anodes. Energy Environ. Sci. *11*, 2600–2608.

15. Wang, J., Huang, W., Pei, A., Li, Y., Shi, F., Yu, X., and Cui, Y. (2019). Improving cyclability of Li metal batteries at elevated temperatures and its origin revealed by cryo-electron microscopy. Nat. Energy *4*, 664–670.

16. Wang, X., Li, Y., and Meng, Y.S. (2018). Cryogenic electron microscopy for characterizing and diagnosing batteries. Joule *2*, 2225–2234.

17. Wang, X., Pawar, G., Li, Y., Ren, X., Zhang, M., Lu, B., Banerjee, A., Liu, P., Dufek, E.J., Zhang, J.-G., et al. (2020). Glassy Li metal anode for high-performance rechargeable Li batteries. Nat. Mater. *19*, 1339–1345.

18. Zachman, M.J., Tu, Z., Choudhury, S., Archer, L.A., and Kourkoutis, L.F. (2018). Cryo-STEM mapping of solid–liquid interfaces and dendrites in lithium-metal batteries. Nature *560*, 345–349.

19. Li, Y., Huang, W., Li, Y., Pei, A., Boyle, D.T., and Cui, Y. (2018). Correlating structure and function of battery interphases at atomic resolution using cryoelectron microscopy. Joule *2*, 2167–2177.

20. Li, Y., Li, Y., Pei, A., Yan, K., Sun, Y., Wu, C.-L., Joubert, L.-M., Chin, R., Koh, A.L., Yu, Y., et al. (2017). Atomic structure of sensitive battery materials and interfaces revealed by cryo–electron microscopy. Science *358*, 506–510.

21. Han, B., Zhang, Z., Zou, Y., Xu, K., Xu, G., Wang, H., Meng, H., Deng, Y., Li, J., and Gu, M. (2021). Poor stability of Li_2CO_3 in the solid electrolyte interphase of a lithium-metal anode revealed by cryo-electron microscopy. Adv. Mater. https://doi.org/10.1002/adma.202100404.

22. Benitez, L., and Seminario, J.M. (2017). Ion diffusivity through the solid electrolyte interphase in lithium-ion batteries. J. Electrochem. Soc. *164*, E3159–E3170.

23. Sarkar, A., Nlebedim, I.C., and Shrotriya, P. (2020). Performance degradation due to anodic failure mechanisms in lithium-ion batteries. J. Power Sources *502*, 229145.

24. Markevich, E., Salitra, G., Chesneau, F., Schmidt, M., and Aurbach, D. (2017). Very stable lithium metal stripping–plating at a high rate and high areal capacity in fluoroethylene carbonate-based organic electrolyte solution. ACS Energy Lett. *2*, 1321–1326.

25. Single, F., Horstmann, B., and Latz, A. (2017). Revealing SEI morphology: in-depth analysis of a modeling approach. J. Electrochem. Soc. *164*, E3132–E3145.

26. He, M., Guo, R., Hobold, G.M., Gao, H., and Gallant, B.M. (2020). The intrinsic behavior of lithium fluoride in solid electrolyte interphases on lithium. Proc. Natl. Acad. Sci. U S A *117*, 73–79.

27. Cheng, X.-B., Zhang, R., Zhao, C.-Z., Wei, F., Zhang, J.-G., and Zhang, Q. (2016). A review of solid electrolyte interphases on lithium metal anode. Adv. Sci. *3*, 1500213.

28. Chen, S., Zheng, J., Yu, L., Ren, X., Engelhard, M.H., Niu, C., Lee, H., Xu, W., Xiao, J., Liu, J., and Zhang, J.-G. (2018). High-efficiency lithium metal batteries with fire-retardant electrolytes. Joule *2*, 1548–1558.

29. Lin, Y.-X., Liu, Z., Leung, K., Chen, L.-Q., Lu, P., and Qi, Y. (2016). Connecting the irreversible capacity loss in Li-ion batteries with the electronic insulating properties of solid electrolyte interphase (SEI) components. J. Power Sources *309*, 221–230.

30. Wang, A., Kadam, S., Li, H., Shi, S., and Qi, Y. (2018). Review on modeling of the anode solid electrolyte interphase (SEI) for lithium-ion batteries. NPJ Comput. Mater. *4*, 15.

31. Nie, M., Demeaux, J., Young, B.T., Heskett, D.R., Chen, Y., Bose, A., Woicik, J.C., and Lucht, B.L. (2015). Effect of vinylene carbonate and fluoroethylene carbonate on SEI formation on graphitic anodes in Li-ion batteries. J. Electrochem. Soc. *162*, A7008–A7014.

32. Heiskanen, S.K., Kim, J., and Lucht, B.L. (2019). Generation and evolution of the solid electrolyte interphase of lithium-ion batteries. Joule *3*, 2322–2333.

33. Suo, L., Xue, W., Gobet, M., Greenbaum, S.G., Wang, C., Chen, Y., Yang, W., Li, Y., and Li, J. (2018). Fluorine-donating electrolytes enable highly reversible 5-V-class Li metal batteries. Proc. Natl. Acad. Sci. U S A *115*, 1156–1161.

34. Lee, J., Kim, Y.-J., Jin, H.S., Noh, H., Kwack, H., Chu, H., Ye, F., Lee, H., and Kim, H.-T. (2019). Tuning two interfaces with fluoroethylene carbonate electrolytes for high-performance Li/LCO batteries. ACS Omega *4*, 3220–3227.

35. Fang, C., Lu, B., Pawar, G., Zhang, M., Cheng, D., Chen, S., Ceja, M., Doux, J.-M., Cai, M., Liaw, B., and Meng, Y.S. (2020). Pressure-tailored lithium deposition and dissolution in lithium metal batteries. arXiv.